EPJ Web of Conferences **84**, 01002 (2015)
DOI: 10.1051/epjconf/20158401002

State selective study of H_3^+ recombination in Cryo-FALP and SA-CRDS experiments at 77 K

Juraj Glosík[a], Michal Hejduk, Petr Dohnal, Peter Rubovič, Ábel Kálosi and Radek Plašil

Charles University in Prague, Faculty of Mathematics and Physics, Department of Surface and Plasma Science, V Holešovičkách 2, 18000 Prague, Czech Republic

Abstract. Rate coefficients for nuclear spin state-specific recombination of H_3^+ ions with thermal electrons were measured using FALP and SA techniques at temperatures 77–300 K. For this purpose H_2 gas with both thermal and enriched population of the para nuclear spin configuration was used. Measurements have shown that at 77 K para-H_3^+ exhibits five times higher binary recombination rate coefficient than ortho-H_3^+: $(1.5 \pm 0.4) \times 10^{-7}$ vs. $(3 \pm 2) \times 10^{-8}$ cm^{3}s^{-1}.

1. Introduction

H_3^+ ion is the most abundantly produced molecular ion in interstellar space [1] and as such stands at the beginnings of astrochemical chains leading to formation of other astrophysically important molecules. One of its major destruction mechanisms, recombination with electrons

$$H_3^+ + e^- \xrightarrow{\alpha_{\mathrm{bin-TDE}}(T)} H_2 + H, H + H + H, \tag{1a}$$

where $\alpha_{\mathrm{bin-TDE}}(T)$ is recombination rate coefficients of H_3^+ ions with population of states according to thermal equilibrium at temperature T, has been studied for more than 60 years [2–4]. Recently, attention has been focused on the dependence of the recombination rate coefficient of H_3^+ ions on nuclear spin states of these ions (para and ortho):

$$^{\mathrm{p}}H_3^+ + e^- \xrightarrow{^{\mathrm{p}}\alpha_{\mathrm{bin}}} H_2 + H, H + H + H \tag{1b}$$

$$^{\mathrm{o}}H_3^+ + e^- \xrightarrow{^{\mathrm{o}}\alpha_{\mathrm{bin}}} H_2 + H, H + H + H, \tag{1c}$$

where "p" and "o" superscripts indicate para and ortho nuclear spin configurations of H_3^+, respectively. The corresponding binary state-specific rate coefficients for pure para-H_3^+ and pure ortho-H_3^+ are $^{\mathrm{p}}\alpha_{\mathrm{bin}}$ and $^{\mathrm{o}}\alpha_{\mathrm{bin}}$, respectively. In the text below we will use $^{\mathrm{p}}f_3$ and $^{\mathrm{o}}f_3$ for relative populations (fractions) of para-H_3^+ and ortho-H_3^+ in H_3^+. The overall recombination rate coefficient is then given by a sum:

$$\alpha_{\mathrm{bin}}\left(^{\mathrm{p}}f_3\right) = {}^{\mathrm{p}}f_3\,{}^{\mathrm{p}}\alpha_{\mathrm{bin}} + {}^{\mathrm{o}}f_3\,{}^{\mathrm{o}}\alpha_{\mathrm{bin}} \tag{2}$$

[a] Corresponding author: juraj.glosik@mff.cuni.cz

for more details see Ref. [5]. The state-specific binary recombination has been studied by monitoring decay of the low temperature H_3^+ dominated afterglow plasma (in He/Ar/H_2 gas mixture) [5–7] and also by several storage ring experiments, see Refs. [8–11]. The advantage of the afterglow experiments is that H_3^+ ions are rotationally thermalized by multiple collisions with ambient neutral gas molecules/atoms at properly chosen conditions [5, 12]. In the recent afterglow type experiments the evolution of densities of H_3^+ ions in the particular spin state and the thermalisation (rotational temperature within para and ortho nuclear spin manifolds and kinetic temperature) are monitored by a laser absorption spectroscopy (SA-CRDS – Stationary Afterglow with Cavity Ring-Down absorption Spectrometer [6, 7, 13]). One of the advantages of plasmatic environment is possibility to study ternary recombination processes assisted by neutrals, by electrons, or eventually by both of them, see Refs. [14–17] and references therein. In studies of binary recombination of H_3^+ ions in He/Ar/H_2 gas mixture it was observed that the decay of afterglow plasma is dependent on He number density [5, 6, 18–20]. This indicates that a ternary He-assisted recombination process contributes to the overall recombination in afterglow plasma in He/Ar/H_2 gas mixture:

$$H_3^+ + e^- + He \xrightarrow{K_{\text{He-TDE}}(T)} \text{neutral products} + He \tag{3a}$$

where $K_{\text{He-TDE}}(T)$ is the ternary recombination rate coefficients of H_3^+ ions with population of states according to thermal equilibrium at temperature T. In this ternary process a dependence of ternary recombination rate coefficient on nuclear spin state of the recombining H_3^+ ions was also observed [5]:

$$^{\text{p}}H_3^+ + e^- + He \xrightarrow{^{\text{p}}K_{\text{He}}} \text{neutral products} + He \tag{3b}$$

$$^{\text{o}}H_3^+ + e^- + He \xrightarrow{^{\text{o}}K_{\text{He}}} \text{neutral products} + He \tag{3c}$$

where $^{\text{p}}K_{\text{He}}$ and $^{\text{o}}K_{\text{He}}$ are corresponding ternary recombination rate coefficients for pure para-H_3^+ and pure ortho-H_3^+, respectively. At low pressure of He we observed a linear dependence of overall (effective) binary recombination rate coefficient α_{eff} on [He]:

$$\alpha_{\text{eff}} = \alpha_{\text{bin}} + K_{\text{He}} \cdot [\text{He}]. \tag{4}$$

The state selective experiments by Dohnal *et al.* [5, 6] and Varju *et al.* [7] have been performed at temperatures 77–200 K using SA-CRDS apparatus. The measurements with SA-CRDS at 77 K have shown that the binary recombination rate coefficient $^{\text{p}}\alpha_{\text{bin}}$ for $^{\text{p}}H_3^+$ is at 77 K approximately 10 times higher than corresponding $^{\text{o}}\alpha_{\text{bin}}$ for $^{\text{o}}H_3^+$ [5]. This difference decreases with increasing temperature up to 200 K, where both binary rate coefficients are comparable. After taking into the account Jahn-Teller effect [21–23], the theoretical calculations were successful in description of the binary recombination processes (1a, 1b, 1c). Measured ternary recombination rate coefficients also showed pronounced nuclear spin specificity at temperatures 100–200 K. Theory of the aforementioned ternary processes is based on a calculation of the life time of rotationaly excited neutral $^{\text{p/o}}H_3$ Rydberg molecule. This molecule is formed in collision of $^{\text{p/o}}H_3^+$ with electron [18–20] and theory predicts the order of magnitude of the ternary rate coefficient correctly. However, the theory is not detailed enough for closer comparison with the experimental values of state selected ternary rate coefficients and their temperature dependencies.

We will show new data in present paper and previous results obtained in SA-CRDS and Cryo-FALP II (Cryogenic Flowing Afterglow with Langmuir Probe) experiments working in conjunction with a source of para-enriched hydrogen gas (para-hydrogen generator) will be summarized. Presented data are deliberately selected from the experiments made at 77 K, where difference between recombination of para- and ortho-H_3^+ is large.

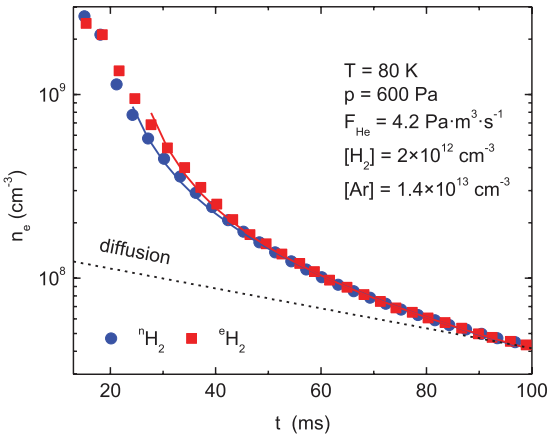

Figure 1. The electron density decay curves measured by Langmuir probe [28] along the flow tube in Cryo-FALP II experiment [16] at 77 K with $^{n}H_2$ (circles) and with $^{e}H_2$ (squares). Hydrogen gas is added to the flow tube at position corresponding to 15 ms. The full lines indicate the fits of the measured data. The dashed line indicates the decay due to losses by ambipolar diffusion. Obtained effective recombination rate coefficients are $\alpha_{eff}(^{n}H_2) = 1.7 \times 10^{-7}\,cm^3s^{-1}$ and $\alpha_{eff}(^{e}H_2) = 2.1 \times 10^{-7}\,cm^3s^{-1}$.

2. Experiments

Cryo-FALP II [16] is a modification of the standard FALP technique [24]. The technical details were described elsewhere [14, 20, 25], only very short description will be given here. A source of para-state-enriched hydrogen gas (para-hydrogen generator) was also described in our previous publication [12]. The combination of the para-hydrogen generator and Cryo-FALP II allows us to measure the recombination rate coefficients of para- and ortho-H_3^+ ions with electrons at temperatures down to 40 K [15, 16]. To obtain information on para/ortho H_3^+ composition in the afterglow plasma, which is important for evaluation of state specific recombination rate coefficients we measured this composition in parallel SA-CRDS experiment at temperatures 77–300 K [5–7, 12]. In the Cryo-FALP II setup the movable Langmuir probe [26] measures the electron number density along the flow tube and the time evolution of electron density in afterglow plasma (see example in Fig. 1) can be obtained [27–29]. A microwave discharge is ignited in helium buffer gas (with a number density [He] ~10^{16}–$10^{17}\,cm^{-3}$) in the first section of the flow tube kept at room temperature and plasma consisting of helium metastable atoms He^m, He^+, and He_2^+ ions and electrons is formed. Downstream at temperature 100 K argon is introduced ([Ar] ~ $10^{13}\,cm^{-3}$) and Ar^+ dominated plasma is formed. The plasma then flows into the section where either normal H_2 ($^{n}H_2$) or para-states-enriched H_2 ($^{e}H_2$) is introduced (typical [H_2] ~ 5×10^{11}–$2 \times 10^{13}\,cm^{-3}$) and H_3^+ dominated plasma is formed. In this article the H_2 with para-H_2 fraction $^{p}f_2 = 0.25$ is denoted as normal H_2 and it is represented by symbol $^{n}H_2$. The symbol $^{e}H_2$ is used for para enhanced H_2 gas. The kinetics of formation of H_3^+ dominated afterglow plasma was described in details in Refs. [27, 29]. Formed H_3^+ ions are thermalized in subsequent multiple collisions with He and H_2. The thermalisation of plasma during the afterglow was studied at similar conditions using SA-CRDS (kinetic energy and rotational temperature [5, 7, 12]).

The para-state-enriched hydrogen gas is produced using "para-hydrogen generator" that works on principle of conversion of $^{o}H_2$ to $^{p}H_2$ on thermally dehydrated $HFeO_2$ surface cooled in cryostat to temperatures 10–18 K [30]. In this experiment normal hydrogen ($^{n}H_2$) is liquefied in the catalyst container and the saturated vapor of converted gas ($^{e}H_2$) is collected through an outlet tube. The actual value of $^{p}f_2$ in $^{e}H_2$ was obtained by measurement of $N^+ + H_2$ reaction rate coefficient in a low temperature ion trap [31]. The outlet tube of para-hydrogen generator is connected to the hydrogen

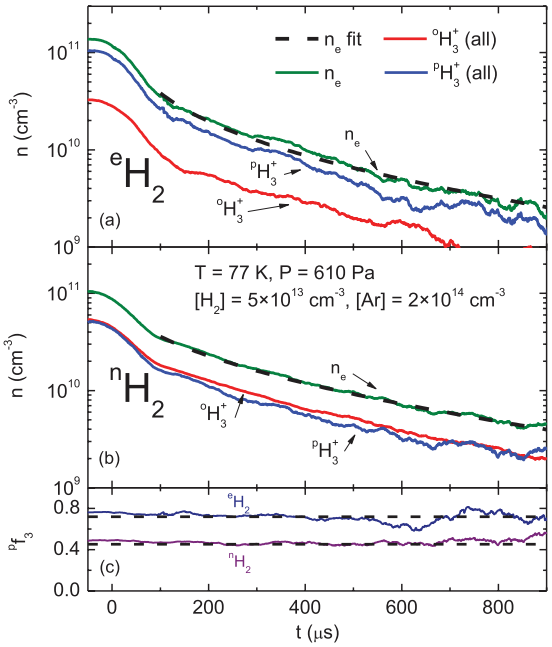

Figure 2. The $^{o}H_3^+$ and $^{p}H_3^+$ number density decay curves measured in SA-CRDS experiment at 77 K with $^{e}H_2$ and with $^{n}H_2$, panels (a) and (b), respectively. Electron number density n_e is calculated as sum of $[^{o}H_3^+]$ and $[^{p}H_3^+]$. The dashed lines indicate the fit of the measured data. Time evolutions of population $^{p}f_3$ of $^{p}H_3^+$ for both $^{n}H_2$ and $^{e}H_2$ are shown in panel (c).

entry port of the Cryo-FALP II apparatus which provide a well-defined and constant flow of para-H_2 with relative population (para fraction of H_2) $^{p}f_2 = (0.995 \pm 0.005)$.

In both experiments the decrease of electron/ion densities during the afterglow was measured. The examples of the decay curves measured in Cryo-FALP II and SA-CRDS experiments are shown in Figs. 1 and 2, respectively. Note large difference in time scale and in electron densities in both experiments. The measured decay curves were fitted to obtain recombination rate coefficients. Using Eq. (4) we can obtain $\alpha_{\mathrm{bin-TDE}}(T)$ and $K_{\mathrm{He-TDE}}(T)$ from the measured dependences of an apparent (effective) recombination rate coefficient α_{eff} on [He] and T. If α_{eff} is measured using hydrogen gas with two different relative populations of $^{p}H_2$, e.g. by using $^{n}H_2$ and $^{e}H_2$, we obtain afterglow plasmas with different relative populations of $^{p}H_3^+$ ($^{p}f_3$). From corresponding decay curves (see Fig. 2) we can obtain dependence of α_{eff} on $^{p}f_3$ and consequently we can calculate $^{p/o}\alpha_{\mathrm{bin}}(T)$ and $^{o/p}K_{\mathrm{He}}(T)$, details of data analysis are given in Refs. [5, 6].

3. Population of para-H_3^+ and ortho-H_3^+ in afterglow plasma

To obtain recombination rate coefficients for H_3^+ ions in thermodynamic equilibrium and for pure para- and ortho-H_3^+ from afterglow experiment one need to know relative population of para-H_3^+ to ortho-H_3^+, i.e. $^{p}f_3$ value. In present study we decided to use dependence $^{p}f_3 = {}^{p}f_3(T, {}^{p}f_2, [\mathrm{He}], [\mathrm{H_2}])$ measured in SA-CRDS experiment. We used both experiments to monitor decay of the afterglow plasma in a He/Ar/H_2 mixture at different temperatures and over a broad range of He and H_2 number densities. In SA-CRDS experiments we monitored also para/ortho composition of H_3^+ ions in afterglow with $^{n}H_2$ and $^{e}H_2$. The fraction $^{p}f_3$ at 77 K was measured very carefully over broad range of $^{n}H_2$, $^{e}H_2$ and He densities. The dependence of $^{p}f_3$ on [He] measured at 77 K is shown in Fig. 3 and the dependence of

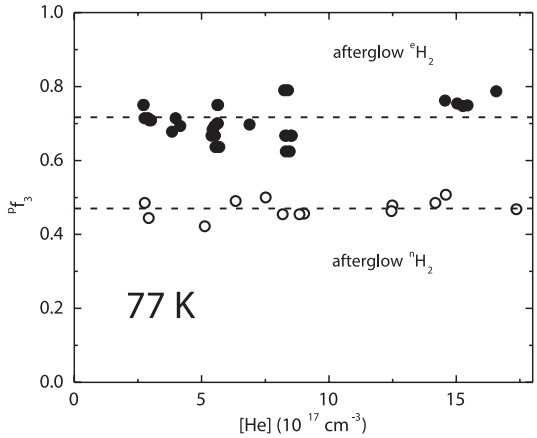

Figure 3. The dependence of the fraction $^{p}f_3$ of para-H_3^+ on He number density in afterglow plasma measured at different number densities of $^{n}H_2$ (empty circles) and $^{e}H_2$ (full circles). Hydrogen number densities were varied in the range 2×10^{13}–5×10^{14} cm^{-3}.

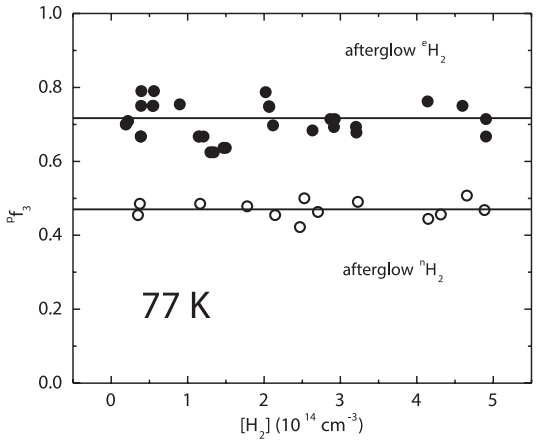

Figure 4. The dependence of the fraction $^{p}f_3$ of para-H_3^+ on hydrogen number density in afterglow plasma measured in experiments with $^{n}H_2$ (empty circles) and $^{e}H_2$ (full circles). The helium number density was varied in the range 2×10^{17}–2×10^{18} cm^{-3}.

$^{p}f_3$ on [H_2] measured at 77 K is shown in Fig. 4. The constant value of $^{p}f_3$(77 K) at broad range of $^{n}H_2$, $^{e}H_2$ and He densities made it possible to use the results from SA-CRDS for analysis of data from Cryo-FALP II. The parameter which was kept the same in both experiments is the number of collisions of formed H_3^+ with H_2 prior to its recombination.

The kinetic temperature of H_3^+ ions T_{Kin} is determined from Doppler broadening of the measured absorption lines in SA-CRDS experiment. From the measured relative populations of H_3^+ ions in ortho (1,0), (3,3), and para (1,1) states we obtained relative population (fraction $^{p}f_3$) of para H_3^+ in the afterglow plasma and also rotational temperature of H_3^+ in ortho manifold ($T_{\mathrm{Rot-ortho}}$) at particular kinetic temperature of the ions. On the basis of our present and previous measurements of T_{Kin} and $T_{\mathrm{Rot-ortho}}$ we concluded that in both afterglow experiments we can use $T_{\mathrm{Rot-ortho}} = T_{\mathrm{Kin}} = T_{\mathrm{He}}$ in rather good approximation (T_{He} is temperature of helium buffer gas). From the measured diffusion losses during the afterglow and also from study of CRR of Ar^+ ions we can write $T_{\mathrm{e}} = T_{\mathrm{He}}$ for electron

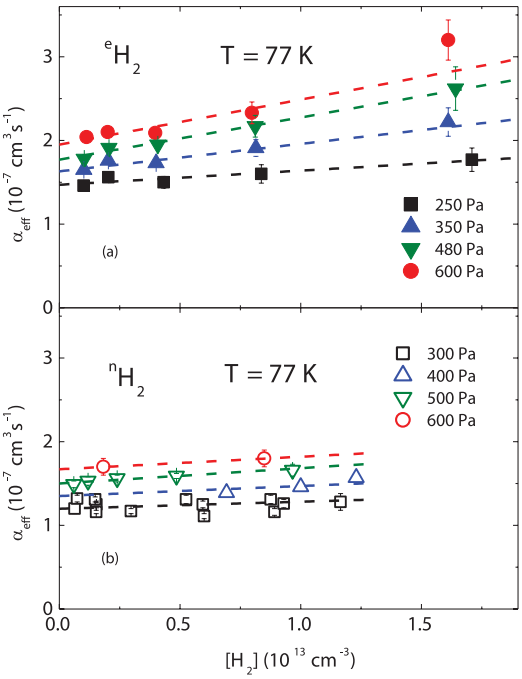

Figure 5. The dependence of α_{eff} on [H_2] measured at several He pressures at 77 K in experiments with $^{e}H_2$ (panel (a)) and with $^{n}H_2$ (panel (b)) Dotted lines represent linear fits of the data.

temperature in good approximation again [14]. If we consider also measurements of $^{p}f_3$ we can conclude that in plasmas containing $^{n}H_2$ ions under study are kinetically and internally thermalized. In plasmas containing $^{e}H_2$ we found that $T_{\text{Rot}-\text{ortho}} = T_{\text{Kin}} = T_{\text{He}}$ but in this case the relative abundances of para-H_3^+ and ortho-H_3^+ ($^{p}f_3$ and $^{o}f_3$) are not according to thermal equilibrium at given T.

4. Measurements of state selected recombination rate coefficients in Cryo-FALP II experiment

By utilizing dependence of $^{p}f_3 = ^{p}f_3(T, ^{p}f_2$, [He], [$H_2$]) obtained in SA-CRDS experiment, state selected recombination rate coefficients can be measured using Cryo-FALP II apparatus. In our previous studies we observed that recombination of H_3^+ ions in He/Ar/H_2 gas mixture is governed by binary and by ternary He assisted processes. When measuring α_{eff} in experiments with $^{e}H_2$ we observed also dependence of α_{eff} on [$^{e}H_2$]. The effective rate coefficients α_{eff} measured at 77 K and several He pressures in Cryo-FALP II experiments with $^{n}H_2$ and $^{e}H_2$ are plotted in Fig. 5. In the first approximation we fitted the data with linear dependence $\alpha_{\text{eff}} \sim \alpha_{\text{effn}-0} + \text{const.}[H_2]$. In experiment with $^{n}H_2$ the dependence on [H_2] is very small (within accuracy of experiment). We deliberately did not write proportionality constant as K_{H2} because from available experimental data we cannot conclude that observed dependence on [$^{e}H_2$] is given by a ternary $^{e}H_2$ assisted recombination. We presume that the dependence can be connected with enhanced formation of H_5^+ in $^{p}H_2$ enriched hydrogen at low temperature [32]. We just assume that at low hydrogen densities the dependence of α_{eff} on [$^{e}H_2$] is in good approximation linear and can be accounted for in the data analysis.

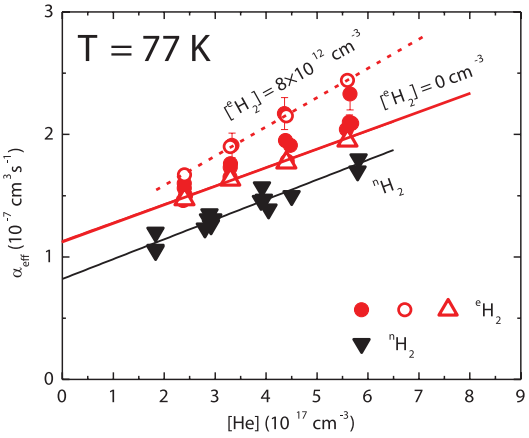

Figure 6. The dependence of α_{eff} on [He] measured at several H_2 densities at 77 K in experiments with $^{n}H_2$ and with $^{e}H_2$ (see Fig. 5). The closed triangles and closed circles indicate data measured in experiments with $^{n}H_2$ and with $^{e}H_2$, respectively. The open circles and the open triangles indicate data obtained from the linear fit in Fig. 5 for $[H_2] = 8 \times 10^{12}\,\mathrm{cm}^{-3}$ and for $[H_2] \to 0$, respectively. The full straight lines indicate the fit of the data (indicated by open and closed triangles) by function $\alpha_{\mathrm{eff}} = \alpha_{\mathrm{bin}} + K_{\mathrm{He}} \cdot [\mathrm{He}]$.

The α_{eff} measured in experiments with $^{n}H_2$ and with $^{e}H_2$ are plotted in Fig. 6 as a function of [He] (closed triangles and circles, respectively). Plotted are also values of $\alpha_{\mathrm{effe-0}}$ (open triangles) obtained from the extrapolation of the measured α_{eff} towards low $[^{e}H_2]$, $\alpha_{\mathrm{effe-0}} = \alpha_{\mathrm{eff}}$ ([He], $[^{e}H_2] \to 0$).

From the linear fit of the data plotted in Fig. 6 we can see that α_{eff} is dependent on $^{p}f_3$ and the dependence of K_{He} on $^{p}f_3$ is only very weak (nearly parallel lines). Statistical errors of measured data are within 5% but systematic error of the measurement itself is about 30%, see detailed discussion in [14]. From the parameters of the fit we obtain the corresponding binary α_{bin} ($^{n}H_2$, 77 K) $= (0.8 \pm 0.3) \times 10^{-7}\,\mathrm{cm}^3\mathrm{s}^{-1}$, α_{bin} ($^{e}H_2$, 77 K) $= (1.2 \pm 0.3) \times 10^{-7}\,\mathrm{cm}^3\mathrm{s}^{-1}$ and ternary rate coefficients are: K_{He} ($^{n}H_2$, 77 K) $= (1.6 \pm 0.5) \times 10^{-25}\,\mathrm{cm}^6\mathrm{s}^{-1}$, K_{He} ($^{e}H_2$, 77 K) $= (1.5 \pm 0.4) \times 10^{-25}\,\mathrm{cm}^6\mathrm{s}^{-1}$. When considering para/ortho composition of H_3^+ we obtained rate coefficients for pure para-H_3^+ and pure ortho-H_3^+: $^{p}\alpha_{\mathrm{bin}}(77\,\mathrm{K}) = (1.5 \pm 0.4) \times 10^{-7}\,\mathrm{cm}^3\mathrm{s}^{-1}$, $^{o}\alpha_{\mathrm{bin}}(77\,\mathrm{K}) = (0.3 \pm 0.2) \times 10^{-7}\,\mathrm{cm}^3\mathrm{s}^{-1}$, $^{p}K_{\mathrm{He}}(77\,\mathrm{K}) = (1.3 \pm 0.4) \times 10^{-25}\,\mathrm{cm}^6\mathrm{s}^{-1}$, $^{o}K_{\mathrm{He}}(77\,\mathrm{K}) = (1.6 \pm 0.5) \times 10^{-25}\,\mathrm{cm}^6\mathrm{s}^{-1}$.

5. Results and discussion

We studied the state selective recombination of para-H_3^+ and ortho-H_3^+ at 77 K using two afterglow experiments: SA-CRDS and Cryo-FALP II. In both experiments we used normal hydrogen ($^{n}H_2$) and para-enriched hydrogen ($^{e}H_2$) produced by para-hydrogen generator. CRDS spectrometer was used to measure fraction $^{p}f_3$ of $^{p}H_3^+$ in recombination dominated afterglow plasma. Cryo-FALP II was used to measure the time evolution of the electron number density during the afterglow. The obtained binary recombination rate coefficients are plotted together with our previous data in Fig. 7. Present value of the binary rate coefficient $\alpha_{\mathrm{bin-TDE}}(77\,\mathrm{K})$ for H_3^+ ions in thermal equilibrium at temperature 77 K and also binary state-specific rate coefficients $^{p}\alpha_{\mathrm{bin}}$ for pure para-H_3^+ and $^{o}\alpha_{\mathrm{bin}}$ for pure ortho- H_3^+ are in agreement with previous data. In addition the new data have higher accuracy given by FALP technique and higher sensitivity of present arrangement of CRDS spectrometer. We fitted all the values of $^{p}\alpha_{\mathrm{bin}}$ and $^{o}\alpha_{\mathrm{bin}}$ with following function:

$$\alpha_{\mathrm{bin}}(T) = A \left(\frac{T}{300\,\mathrm{K}} \right)^{B} \exp\left(-\frac{C}{T} \right) \tag{5}$$

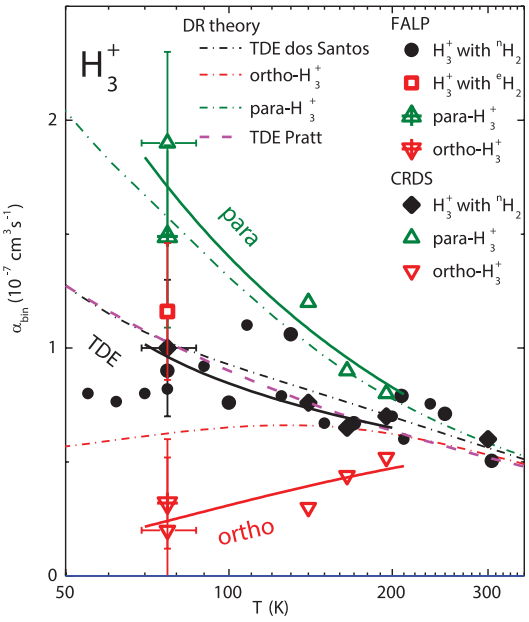

Figure 7. Temperature dependence of nuclear spin state-specific binary recombination rate coefficients measured by Cryo-FALP II and SA-CRDS apparatuses with para-hydrogen generator. Closed circles and closed rhomboids indicate values of ${}^{n}\alpha_{eff}$ measured with Cryo-FALP II [25] and SA-CRDS [5] using ${}^{n}H_2$, respectively. These ${}^{n}\alpha_{bin}$ correspond at 77–300 K to $\alpha_{bin-TDE}$. Open up triangles indicate measured values of ${}^{p}\alpha_{bin}$ and open down triangles indicate values ${}^{o}\alpha_{bin}$, both of them are taken from [5] and [7]. Open square indicate value ${}^{e}\alpha_{bin}$ measured by Cryo-FALP II with para-enriched H_2. The crossed triangles indicate value measured by Cryo-FALP II at 77 K. The full lines indicated as para, ortho and TDE are fits of ${}^{p}\alpha_{bin}$, ${}^{o}\alpha_{bin}$ and corresponding calculated value of $\alpha_{bin-TDE}$. Dash-dotted lines represent theoretical calculations by Fonseca dos Santos [21] for ${}^{o}H_3^+$, ${}^{p}H_3^+$, and H_3^+ with states populated according to TDE. Dashed line represents values of $\alpha_{bin-TDE}$ based on theory by Pratt and Jungen [33].

where A, B, C are free parameters. From the fit functions we calculated corresponding values $\alpha_{bin-TDE}(T)$ for ${}^{p}H_3^+$ and ${}^{o}H_3^+$ in thermal equilibrium (see Fig. 7). These fits are plotted as full lines in Fig. 7. We included also the theoretical dependencies calculated by Fonseca dos Santos *et al.* [21] and by Pratt and Jungen [33] in Fig. 7. Line indicated as theory of Pratt and Jungen in Fig. 7 was calculated from the dependence of the recombination rate on energy [33]. For rate coefficients ${}^{p}\alpha_{bin}$, and $\alpha_{bin-TDE}$ is the agreement of the measured and calculated rate very good for temperatures 77–300 K. The measured ${}^{o}\alpha_{bin}$ is substantially lower in comparison with calculated values. For this conclusion the present Cryo-FALP study with higher accuracy is substantial.

Further measurements extending temperature range are in progress. Presented values of state-selected recombination rate coefficients obtained in Cryo-FALP II experiment are in a very good agreement with previous SA-CRDS results. Nevertheless, as history of H_3^+ recombination has shown, agreement with independent storage ring experiment is desirable.

This work was partly supported by GACR (205/09/1183, P209/12/0233), SV 267 302, and by GAUK 659112.

References

[1] T. Oka, Proc. Natl. Acad. Sci. USA **103**, 12239 (2006)
[2] T. Oka, *Dissociative Recombination of Molecular Ions with* Electrons (Kluwer Academic/Plenum Publishers, New York, 2003)
[3] M. Larsson, A. Orel, *Dissociative Recombination of Molecular* Ions, (Cambridge University Press, Cambridge, 2008)
[4] R. Johnsen, S.L. Guberman, Adv. At. Mol. Opt. Phys. **59**, 75 (2010)
[5] P. Dohnal, M. Hejduk, J. Varju, P. Rubovic, S. Roucka, T. Kotrik, R. Plasil, J. Glosik, R. Johnsen, J. Chem. Phys. **136**, 244304 (2012)
[6] P. Dohnal, M. Hejduk, J. Varju, P. Rubovic, S. Roucka, T. Kotrik, R. Plasil, R. Johnsen, J. Glosik, Phil. T. Roy. Soc. A **370**, 5101 (2012)
[7] J. Varju, M. Hejduk, P. Dohnal, M. Jilek, T. Kotrik, R. Plasil, D. Gerlich, J. Glosik, Phys. Rev. Lett. **106**, 203201 (2011)
[8] H. Kreckel, M. Motsch, J. Mikosch, J. Glosik, R. Plasil, S. Altevogt, V. Andrianarijaona, H. Buhr, J. Hoffman, L. Lammich, M. Lestinsky, I. Nevo, S. Novotny, D.A. Orlov, H.B. Pedersen, F. Sprenger, A.S.Terekhov, J. Toker, R. Wester, D. Gerlich, D. Schwalm, A. Wolf, D. Zajfman, Phys. Rev. Lett. **95**, 2633201 (2005)
[9] B.J. McCall, A.J. Honeycutt, R.J. Saykally, T.R. Geballe, N. Djuric, G.H. Dunn, J. Semaniak, O. Novotny, A. Al-Khalili, A. Ehlerding, F. Hellberg, S. Kalhori, A. Neau, R. Thomas, F. Osterdahl, M. Larsson, Nature **422**, 500 (2003)
[10] B.A. Tom, V. Zhaunerchyk, M.B. Wiczer, A.A. Mills, K.N. Crabtree, M. Kaminska, W.D. Geppert, M. Hamberg, M. af Ugglas, E. Vigren, W.J. van der Zande, M. Larsson, R.D. Thomas, B.J. McCall, J. Chem. Phys **130**, 031101 (2009)
[11] H. Kreckel, O. Novotny, K.N. Crabtree, H. Buhr, A. Petrignani, B.A. Tom, R.D. Thomas, M.H. Berg, D. Bing, M. Grieser, C. Krantz, M. Lestinsky, M.B. Mendes, C. Nordhorn, R. Repnow, J. Stutzel, A. Wolf, B.J. McCall, Phys. Rev. A **82**, 042715 (2010)
[12] M. Hejduk, P. Dohnal, J. Varju, P. Rubovic, T. Kotrik, R. Plasil, J. Glosik, Plasma Sources Sci. Technol. **21,** 024002 (2012)
[13] P. Macko, G. Bano, P. Hlavenka, R. Plasil, V. Poterya, A. Pysanenko, O. Votava, R. Johnsen, J. Glosik, Int. J. Mass Spectrom. **233**, 299 (2004)
[14] P. Dohnal, P. Rubovic, T. Kotrik, M. Hejduk, R. Plasil, R. Johnsen, J. Glosik, Phys. Rev. A **87**, 052716 (2013)
[15] T. Kotrik, P. Dohnal, S. Roucka, P. Jusko, R. Plasil, J. Glosik, R. Johnsen, Phys. Rev. A **83**, 032720 (2011)
[16] T. Kotrik, P. Dohnal, P. Rubovic, R. Plasil, S. Roucka, S. Opanasiuk, J. Glosik, Eur. Phys. J. Appl. Phys. **56**, 24011 (2011)
[17] R.J. Saykally, E.A. Michael, J. Wang, C.H. Greene, J. Chem. Phys. **133**, 234302 (2010)
[18] J. Glosik, I. Korolov, R. Plasil, O. Novotny, T. Kotrik, P. Hlavenka, J. Varju, I.A. Mikhailov, V. Kokoouline, C.H. Greene, J. Phys. B-At. Mol. Opt. **41**, 191001 (2008)
[19] J. Glosik, R. Plasil, I. Korolov, T. Kotrik, O. Novotny, P. Hlavenka, P. Dohnal, J. Varju, V. Kokoouline, C.H. Greene, Phys. Rev. A **79**, 052707 (2009)
[20] R. Johnsen, P. Rubovic, P. Dohnal, M. Hejduk, R. Plasil, J. Glosk, J. Phys. Chem. A **117**, 9477 (2013)
[21] S. Fonseca dos Santos, V. Kokoouline, C.H. Greene, J. Chem. Phys. **127**, 124309 (2007)
[22] C. Jungen, S.T. Pratt, Phys. Rev. Lett. **102**, 023201 (2009)
[23] L. Pagani, C. Vastel, E. Hugo, V. Kokoouline, C.H. Greene, A. Bacmann, E. Bayet, C. Ceccarelli, R. Peng, S. Schlemmer, Astron. Astrophys. **494**, 623 (2009)
[24] J. Glosik, G. Bano, R. Plasil, A. Luca, P. Zakouril, Int. J. Mass Spectrom. **189**, 103 (1999)

[25] P. Rubovic, P. Dohnal, M. Hejduk. R. Plasil, J. Glosik, J. Phys. Chem. A **117**, 9626 (2013)
[26] J.D. Swift, M.J.R. Schwar, *Electrical Probes for Plasma Diagnostics* (Iliffe, London, 1970)
[27] R. Plasil, J. Glosik, V. Poterya, P. Kudrna, J. Rusz, M. Tichy, A. Pysanenko, Int. J. Mass Spectrom. **218**, 105 (2002)
[28] I. Korolov, T. Kotrik, R. Plasil, J. Varju, M. Hejduk, J. Glosik, Contrib. Plasma Phys. **48**, 521 (2008)
[29] J. Glosik, R. Plasil, T. Kotrik, P. Dohnal, J. Varju, M. Hejduk, I. Korolov, S. Roucka, V. Kokoouline, Molec. Phys. **108**, 2253 (2010)
[30] E. Ilisca, Prog. Surf. Sci. **41**, 217 (1992)
[31] I. Zymak, M. Hejduk, D. Mulin, R. Plasil, J. Glosik, D. Gerlich, Astrophys. J. **768**, 86 (2013)
[32] E. Hugo, O. Asvany, S. Schlemmer, J. Chem. Phys. **130**, 164302 (2009)
[33] S.T. Pratt, C. Jungen, J. Phys.: Conf. Ser. **300**, 012019 (2011)